

Supplemental tables

Supplementary Table 1: Genome assembly statistics

step	# scaffolds	N50, Kb	% gap	BUSCO
10xGenomics, Supernova2	174165	33.877	3.073	C:62.9%[S:56.0%,D:6.9%],F:21.0%,M:16.1%,n:3950
Agouti with RNAseq	171284	35.23	8.804	C:64.7%[S:58.2%,D:6.5%],F:19.2%,M:16.1%,n:3950
Jelly on Nanopore	163793	40.024	7.147	C:67.6%[S:61.4%,D:6.2%],F:17.9%,M:14.5%,n:3950
Dovetail	39223	227.932		C:78.6%[S:73.7%,D:4.9%],F:6.4%,M:15.0%,n:5310

Supplementary Table 2: Transcriptome assembly statistics

sample	organ	# raw reads	# transcripts	# transcripts_1tpm_cutoff	after cdhit
AK393	stomach	101,419,756	211105	61363	53092
AK4334	lung	99,048,832	246972	86823	73408
AK2340	skin	155,144,638	290666	84145	71437
AK3438	eye	151,860,400	364970	88779	76814
AK626	brain	142,942,536	621519	169862	152663
merged	-	-	-	490972	228525

Supplementary Table 3: Gene family expansion/contraction

[https://figshare.com/articles/dataset/Changes in cell cycle machinery as genetic basis for polyploidy stabilization in Australian burrowing frogs Neobatrachus /30576644?file=59724149](https://figshare.com/articles/dataset/Changes_in_cell_cycle_machinery_as_genetic_basis_for_polyploidy_stabilization_in_Australian_burrowing_frogs_Neobatrachus_/30576644?file=59724149)

Supplementary Table 4: Sample overview

[https://figshare.com/articles/dataset/Changes in cell cycle machinery as genetic basis for polyploidy stabilization in Australian burrowing frogs Neobatrachus /30576644?file=59724158](https://figshare.com/articles/dataset/Changes_in_cell_cycle_machinery_as_genetic_basis_for_polyploidy_stabilization_in_Australian_burrowing_frogs_Neobatrachus_/30576644?file=59724158)

Supplementary Table 5: ABBA-BABA statistics

D	JK.D	V.JK.D.	Z	pvalue	nABBA	nBABA	nBlocks	H1	H2	H3	H4
-0.226253	-0.226253	8.00E-06	-78.910464	0	46711.21526	74029.13753	386	Nfulvus	Npictus	Nalbipes	Ldumerilli
0.109512	0.109512	1.00E-05	34.945628	0	69308.81975	55626.91236	386	Nsutor	Nwilsmorei	Nalbipes	Ldumerilli
0.085891	0.085891	1.90E-05	19.680214	0	74707.59391	62889.27748	386	Nalbipes	Nsutor	Nfulvus	Ldumerilli
0.034171	0.034171	1.20E-05	9.873014	0	63918.33891	59694.3127	386	Nalbipes	Nwilsmorei	Nfulvus	Ldumerilli
-0.065735	-0.065735	1.30E-05	-18.474778	0	50271.91652	57346.16222	386	Nsutor	Nwilsmorei	Nfulvus	Ldumerilli
-0.258839	-0.258839	8.00E-06	-89.660025	0	51184.83882	86935.81157	386	Nalbipes	Nfulvus	Npelobatooides	Ldumerilli

-0.393355	-0.393355	6.00E-06	-161.085107	0	46429.20843	106639.465	386	Nalbipes	Npictus	Npelobatooides	Ldumerilli
-0.112212	-0.112212	9.00E-06	-36.556505	0	58208.06246	72922.46474	386	Nalbipes	Nsutor	Npelobatooides	Ldumerilli
-0.068212	-0.068212	1.00E-05	-21.302818	0	56950.80332	65289.03872	386	Nalbipes	Nwilsmorei	Npelobatooides	Ldumerilli
-0.210298	-0.210298	8.00E-06	-75.783093	0	43114.9258	66077.92321	386	Nfulvus	Npictus	Npelobatooides	Ldumerilli
0.155947	0.155947	1.30E-05	43.539373	0	77534.6372	56614.53315	386	Nfulvus	Nsutor	Npelobatooides	Ldumerilli
0.195389	0.195389	1.20E-05	55.585044	0	80246.52704	54013.6124	386	Nfulvus	Nwilsmorei	Npelobatooides	Ldumerilli
0.295672	0.295672	8.00E-06	102.027653	0	97668.57858	53092.66628	386	Npictus	Nsutor	Npelobatooides	Ldumerilli
0.325074	0.325074	8.00E-06	113.067445	0	98769.93356	50308.44571	386	Npictus	Nwilsmorei	Npelobatooides	Ldumerilli
0.056898	0.056898	8.00E-06	20.766556	0	54382.79289	48527.41263	386	Nsutor	Nwilsmorei	Npelobatooides	Ldumerilli
0.023321	0.023321	1.70E-05	5.697195	0	60889.18677	58113.97111	386	Nalbipes	Nsutor	Npictus	Ldumerilli
4.00E-04	4.00E-04	1.20E-05	0.116023	0.907	54703.23753	54659.51581	386	Nalbipes	Nwilsmorei	Npictus	Ldumerilli
-0.030258	-0.030258	1.20E-05	-8.561145	0	44947.39298	47752.28171	386	Nsutor	Nwilsmorei	Npictus	Ldumerilli
-0.281701	-0.281701	8.00E-06	-101.132443	0	46440.85217	82866.92962	386	Nfulvus	Npictus	Nsutor	Ldumerilli
-0.246299	-0.246299	8.00E-06	-89.452657	0	45067.07887	74521.65282	386	Nfulvus	Npictus	Nwilsmorei	Ldumerilli

Supplementary Table 6: Pseudohaplotype assignments of tetraploids to the diploid species of origin

Nkunapalari					
pseudohaplotype 1	pseudohaplotype 2	occurrence	occurrence / total	occurrence / known	
Npictus	Npictus	14	0,00475	0,010550113	
Nalbipes	Nfulvus	721	0,24457	0,543330821	
Nalbipes	Nalbipes	211	0,07157	0,159005275	
Nalbipes	Nwilsmorei	26	0,00882	0,019593067	
Nalbipes	Nsutor	122	0,04138	0,091936699	
Nfulvus	Npictus	6	0,00204	0,004521477	
Nalbipes	Npictus	136	0,04613	0,102486812	
Nfulvus	Nfulvus	13	0,00441	0,009796534	
Npelobatooides	Npictus	2	0,00068	0,001507159	
Npelobatooides	Npelobatooides	7	0,00237	0,005275057	
Nsutor	Nsutor	21	0,00712	0,01582517	
Npictus	Nsutor	11	0,00373	0,008289375	
Nsutor	Nwilsmorei	13	0,00441	0,009796534	
Npictus	Nwilsmorei	3	0,00102	0,002260739	
Nalbipes	Npelobatooides	2	0,00068	0,001507159	
Nwilsmorei	Nwilsmorei	1	0,00034	0,00075358	
Nfulvus	Nsutor	14	0,00475	0,010550113	

Nfulvus	Nwilsmorei	4	0,00136	0,003014318
unknown		1621	0,54986	
known		1327	0,45014	
total		2948	1,00000	

Nsudellae

pseudohaplotype 1	pseudohaplotype 2	occurrence	occurrence / total	occurrence / known
Nfulvus	Nsutor	21	0,00560	0,009446694
Nfulvus	Nfulvus	1691	0,45069	0,760683761
Nfulvus	Npictus	76	0,02026	0,034188034
Npictus	Npictus	331	0,08822	0,148897886
Nsutor	Nsutor	65	0,01732	0,029239766
Npictus	Nsutor	8	0,00213	0,00359874
Nalbipes	Nalbipes	17	0,00453	0,007647323
Npelobatoides	Npictus	5	0,00133	0,002249213
Npelobatoides	Npelobatoides	3	0,00080	0,001349528
Nalbipes	Npictus	2	0,00053	0,000899685
Nwilsmorei	Nwilsmorei	2	0,00053	0,000899685
Nalbipes	Nfulvus	1	0,00027	0,000449843
Nfulvus	Npelobatoides	1	0,00027	0,000449843
	unknown	1529	0,40752	
	known	2223	0,59248	
	total	3752	1,00000	

Naqulonius

pseudohaplotype 1	pseudohaplotype 2	occurrence	occurrence / total	occurrence / known
Nfulvus	Npictus	42	0,02238806	0,032735776

Nfulvus	Nfulvus	1069	0,569829424	0,833203429
Nalbipes	Nfulvus	1	0,000533049	0,000779423
Npictus	Nsutor	10	0,00533049	0,007794232
Nfulvus	Nsutor	113	0,060234542	0,088074825
Nfulvus	Nwilsmorei	4	0,002132196	0,003117693
Npictus	Npictus	19	0,010127932	0,014809041
Nsutor	Nsutor	17	0,009061834	0,013250195
Nalbipes	Nwilsmorei	1	0,000533049	0,000779423
Nalbipes	Nsutor	1	0,000533049	0,000779423
Nsutor	Nwilsmorei	4	0,002132196	0,003117693
Nalbipes	Nalbipes	2	0,001066098	0,001558846
	unknown	593	0,316098081	
	known	1283	0,683901919	
	total	1876	1	

Supplementary Table 7:

https://figshare.com/articles/dataset/Changes_in_cell_cycle_machinery_as_genetic_basis_for_polyploid_stabilization_in_Australian_burrowing_frogs_Neobatrachus_/30576644?file=60781930

Supplementary Table 8: Annotated genes that were under selection in all three tetraploid species.

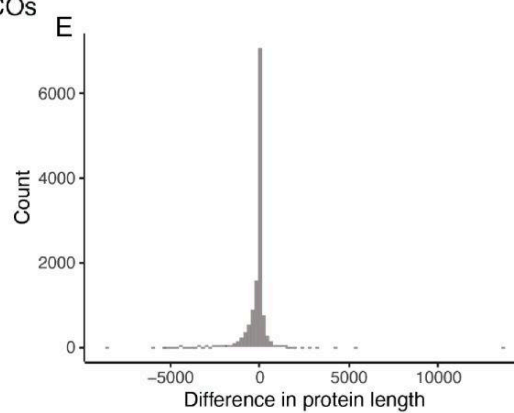
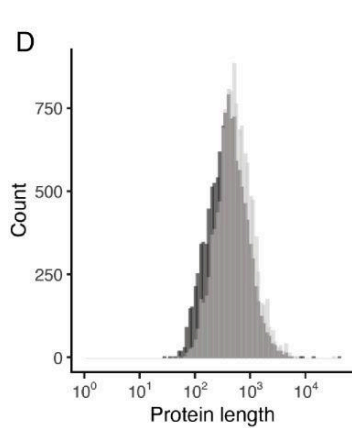
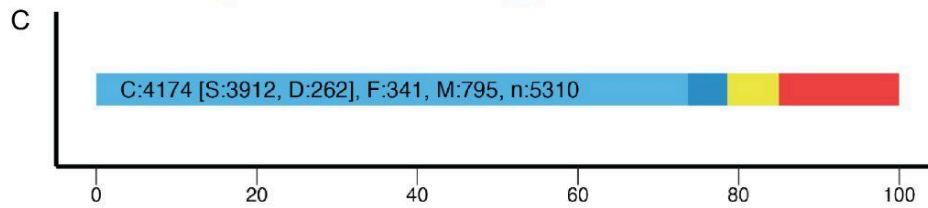
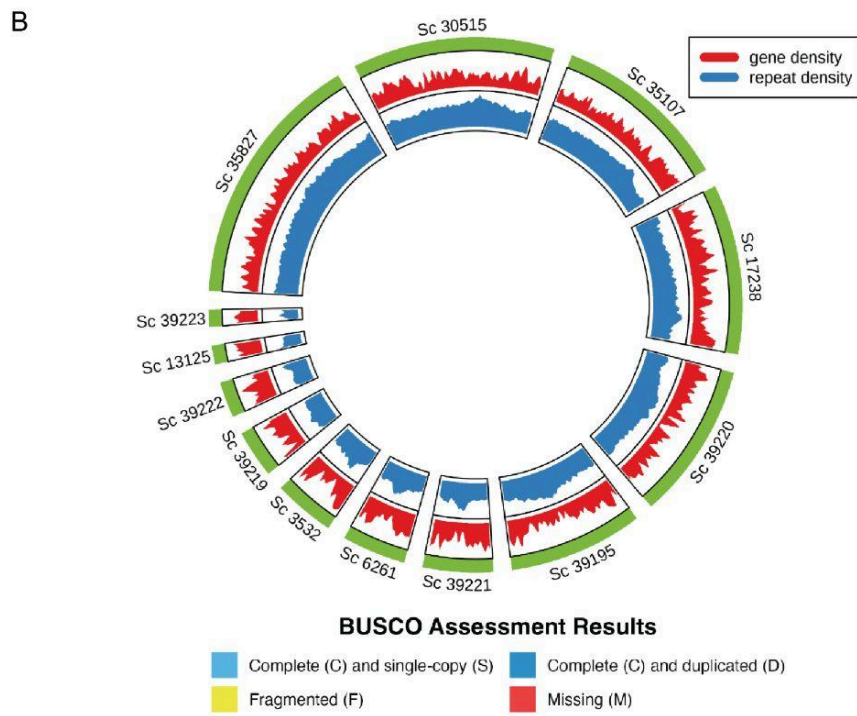
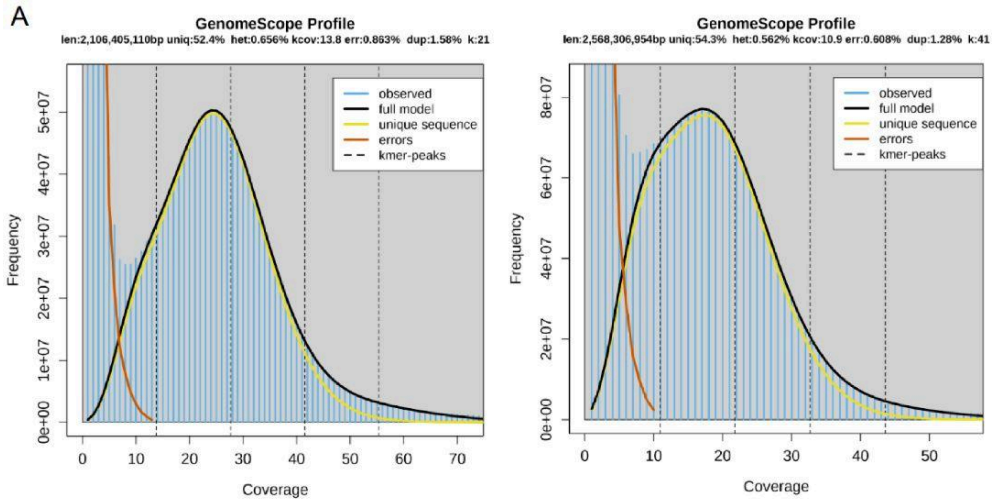
Functional group	Gene	Annotation	GO category
Crossover interference	g5917	SYCE2	synaptonemal complex assembly, structural unit of the synaptonemal complex
	g5068	Proline-rich protein 19	–
Chromosome packaging	g23417	Condensin-2 complex subunit D3	nuclear condensin complex, mitotic chromosome condensation
	g16961	Histone H2A	nucleosome, protein heterodimerization activity, DNA binding
	g5964	Histone H2B	nucleosome, protein heterodimerization activity, DNA binding
	g5970	Histone H3/CENP-A	nucleosome, protein

			heterodimerization activity, DNA binding
Spindle assembly	g2400	Kinesin-14 motor protein KifC1	DNA binding
	g11479	Tetratricopeptide repeat protein 34	
Other	g1430	Pancreatic trypsin inhibitor Kunitz domain	serine-type endopeptidase inhibitor activity
	g1431	Lipocalin/cytosolic fatty-acid binding domain	small molecule binding
	g1506	Allograft inflammatory factor 1	
	g22785	TAF1D	RNA polymerase transcription factor SL1 complex
	g23303	EMI domain profile	
	g23322	BolA protein	
	g23338	Iodothyronine deiodinase	thyroxine 5'-deiodinase activity
	g23627	1-phosphatidylinositol 4,5-bisphosphate phosphodiesterase eta-1	phosphatidylinositol-mediated signaling
	g9063	Glycosyl transferase, family 3	galactosyltransferase activity

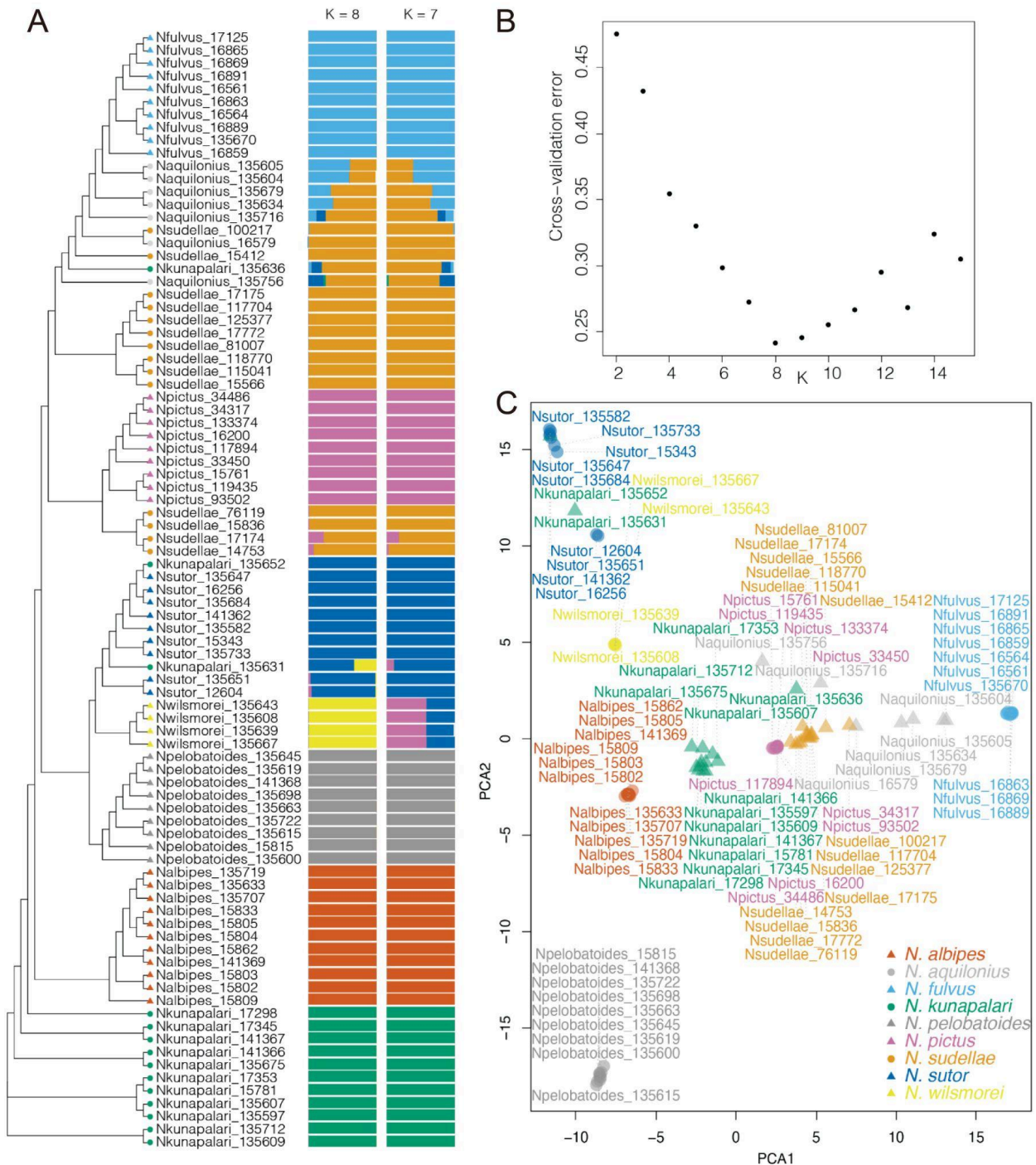
Supplementary Table 9: Introgression genes among tetraploid species.

[https://figshare.com/articles/dataset/Changes in cell cycle machinery as genetic basis for ployploidy stabilization in Australian burrowing frogs Neobatrachus /30576644?file=63103585](https://figshare.com/articles/dataset/Changes_in_cell_cycle_machinery_as_genetic_basis_for_ployploidy_stabilization_in_Australian_burrowing_frogs_Neobatrachus_/30576644?file=63103585)

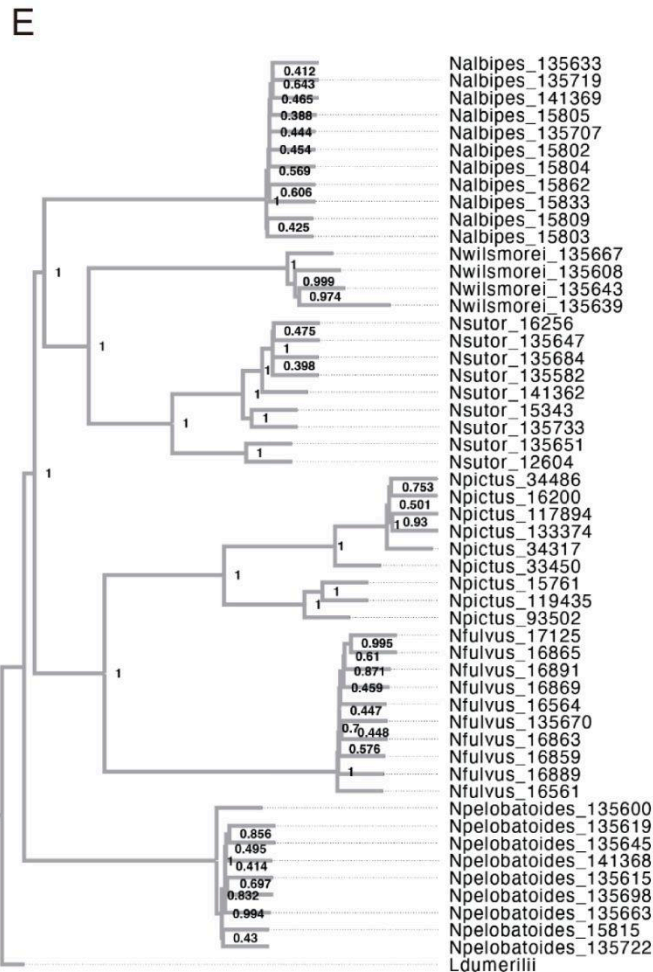
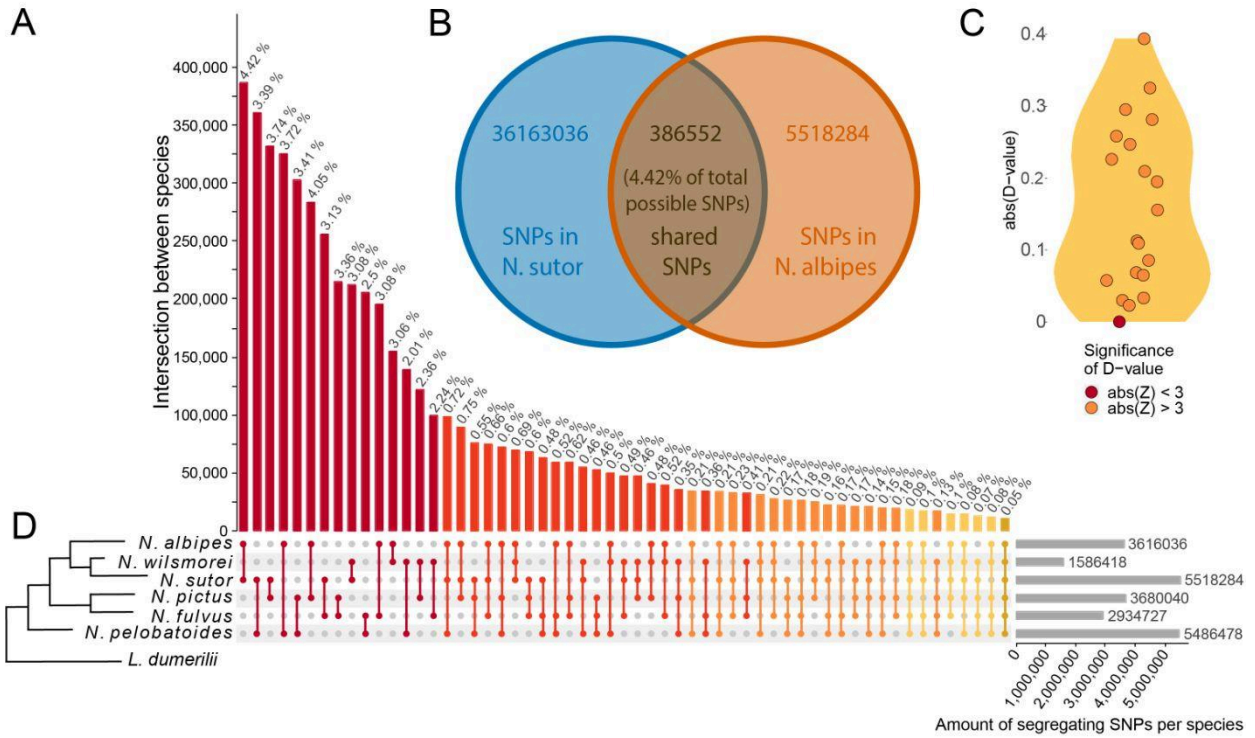
Supplemental figures



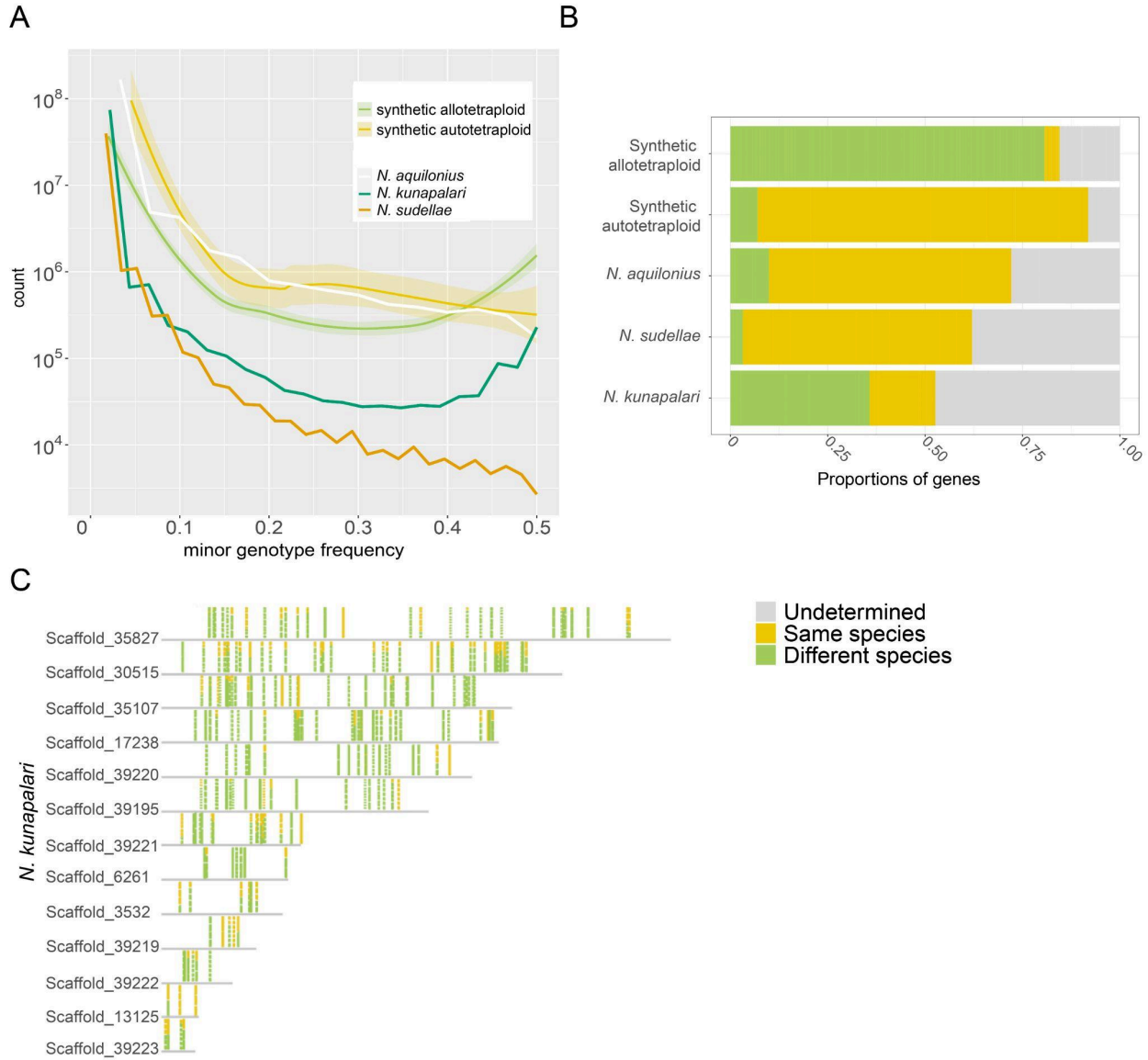
Supplementary Figure 1. A Genome size estimation of *N. pictus* based on k-mer histograms generated by JellyFish. Estimated genome size ranges from 2,106,405,110 to 2,568,306,954 (k-mer = 21-41). Estimation by Genomescope with k-mer = 21 (left) and k-mer = 41 (right). **B.** Gene and repeat density along the 13 biggest scaffolds of *N. pictus*. **C.** BUSCO Assessment results of the assembly of *N. pictus*. **D.** Protein length distribution of *N. pictus* and *X. tropicalis*. **E.** Comparison of protein length of *N. pictus* and *X. tropicalis*. Performed by blastp analysis of *N. pictus* against *X. tropicalis*. Proteins were filtered for $evalue < 0.0001$ and $pident > 0.7$, retaining 12451 of the original 22811 hits.



Supplementary Figure 2. A. Unrooted Neighbour-joining tree of neutral (4fds) sites, accompanied by admixture results for K=8 and K=7 . **B.** Cross Validation error for ADMIXTURE results amount of clusters (K) between 2 and 14. **C.** Principal component analysis of variation on 4fds. Tetraploid individuals are circles, diploid individuals are triangles.

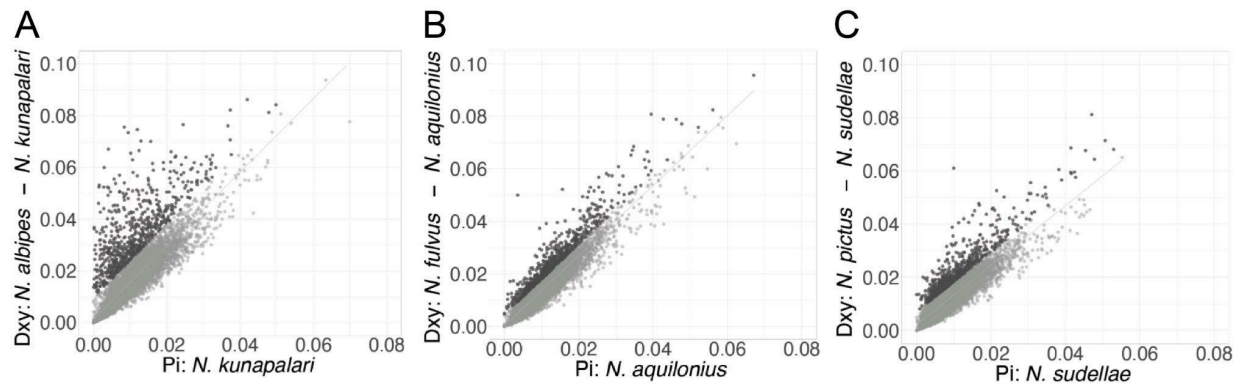


Supplementary Figure 3. **A.** UpSet plot showing the number of shared biallelic single nucleotide polymorphisms (SNPs) between diploid *Neobatrachus* species. The color from dark red to light orange indicates the number of species sharing SNPs from two (dark red) to three, four, five, or all six (light orange) diploid species. Bars are ordered in descending order based on the number of shared SNPs (i.e., intersection region shown in B), and labeled with the percentage of shared SNPs out of the total SNPs (intersection/union) found in the compared species. The horizontal bar plot on the right shows the total number of biallelic SNPs present in each species. **B.** Venn diagram showing how shared SNPs (intersection) are identified in genic regions between a pair of species. The numbers shown here correspond to the first bar on the vertical barplot. **C.** D-statistics from ABBA-BABA analysis for the six diploid *Neobatrachus* species. Each possible combination in concordance with the species tree in Fig. 3F is reported. D-statistics are considered significant if the Z-score is greater than 3 or lower than -3. **D.** Tree topology of the diploid *Neobatrachus* species is shown on the left. The eastern banjo frog, *Limnodynastes dumerilii dumerilii*, was used as an outgroup. **E.** Consensus tree of 385 gene trees of all diploid *Neobatrachus* individuals and *Limnodynastes dumerilii*, based on the maximum number of quartet topologies in the gene trees, weighted by gene tree discordance, constructed using ASTER¹⁵⁸ (v1.15.2.3) and visualized using FigTree (v.1.4.4). Node labels indicate the percentage of quartets among the gene trees that agree with the branch. **F.** Densitree of 385 gene trees of all diploid *Neobatrachus* individuals and outgroup *Limnodynastes dumerilii*.

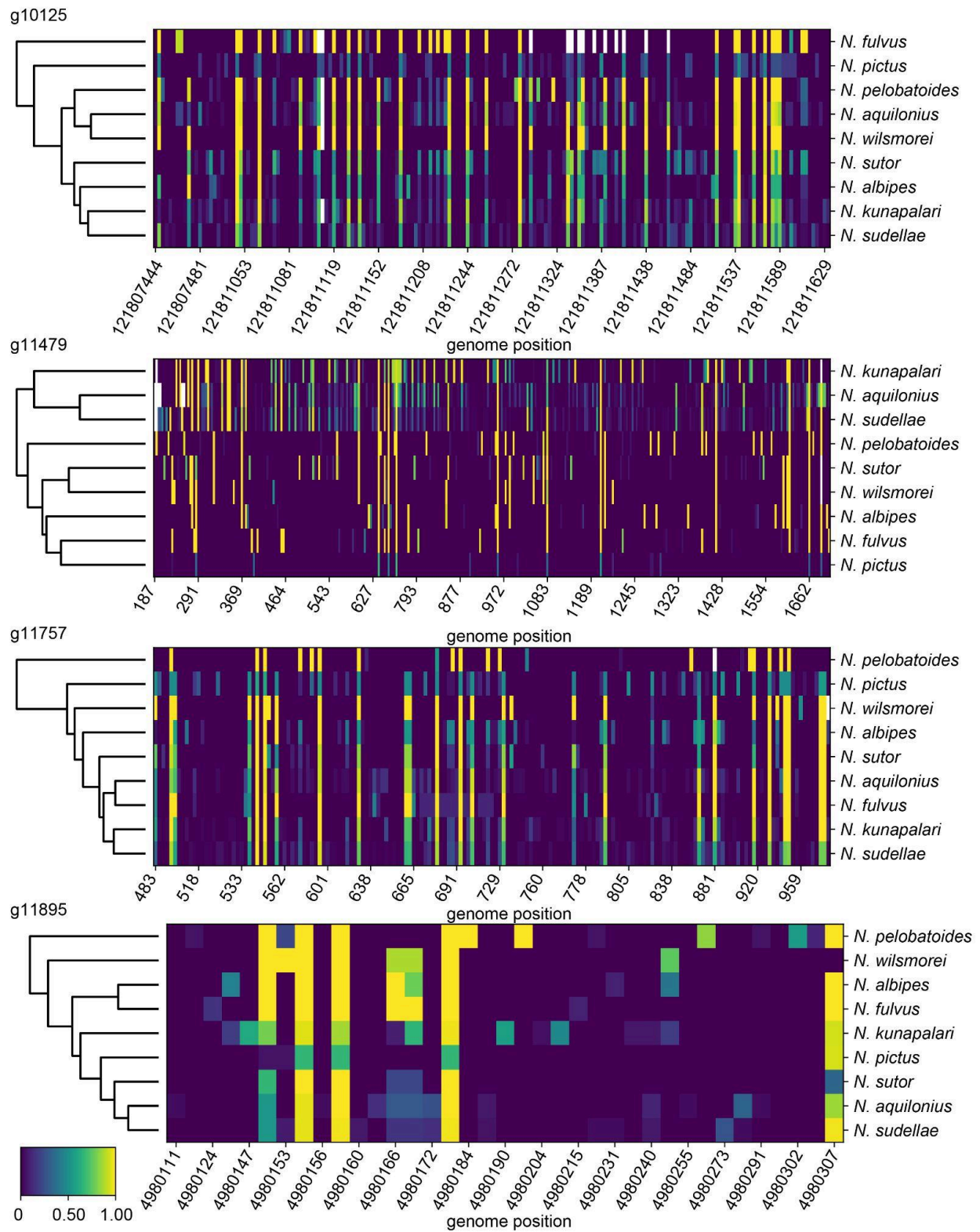


Supplementary Figure 4. A. Site frequency spectra of natural tetraploid *N. sudellae*, *N. aquilonius* and *N. kunapalari* in comparison with synthetic auto- and allotetraploids constructed *in silico* from the diploid species combinations. Synthetic allotetraploid populations exhibit a pronounced peak at intermediate frequency when mapped to a diploid reference due to fixed divergence between the diploid species, while autotetraploid populations do not. The shape of the site frequency spectra of the natural tetraploid *N. sudellae* and *N. aquilonius* resembles synthetic autotetraploids, while *N. kunapalari* shows an increase of minor genotype counts at 0.5 frequencies similar to synthetic allotetraploids. **B.** Overall phylogenetic assignment of natural and synthetic tetraploid pseudohaplotypes to the matching or discordant diploid species. **C.** Species-wide phylogenetic assignment of pseudohaplotypes of *N. kunapalari* to the matching (yellow) or discordant (green) diploid species along the genome. Each individual sample from *N. kunapalari* was assigned matching or discordant parental haplotypes, together forming a dotted bar at each locus. The dots correspond to an assignment of one individual at this locus. None of the longest scaffolds (chromosomes) are consistently assigned to matching (yellow) or discordants (green) parents,

suggesting that *N. kunapalari* has mixed inheritance mode and homeologs can recombine throughout the genome.

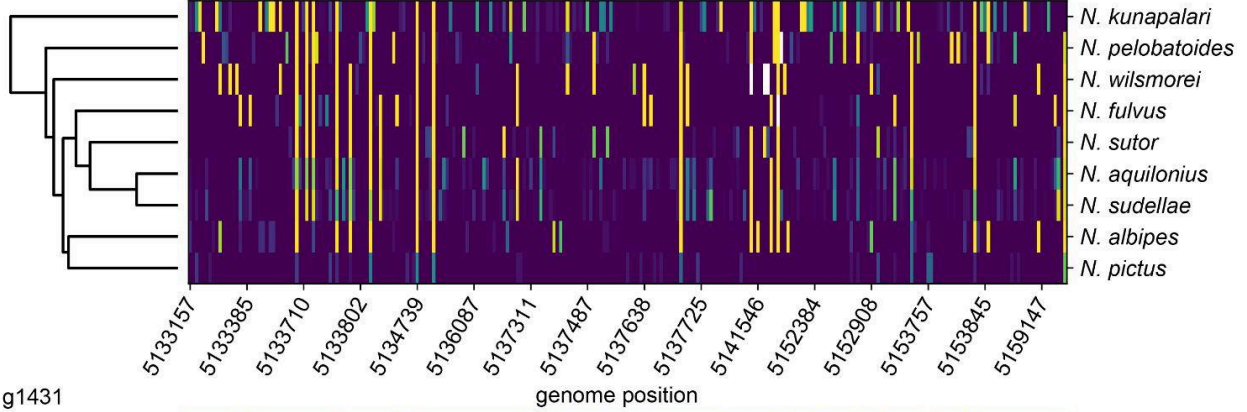


Supplementary Figure 5. Scatterplots showing the relationship between nucleotide diversity within tetraploid species and nucleotide divergence per diploid–tetraploid species pair per gene: (A) 2n *N. albipes* - 4n *N. kunapalari*; (B) 2n *N. fulvus* - 4n *N. aquilonius*; (C) 2n *N. pictus* - *N. sudellae*. The top 5% residual outliers from linear regression (gray line) are denoted in dark gray.

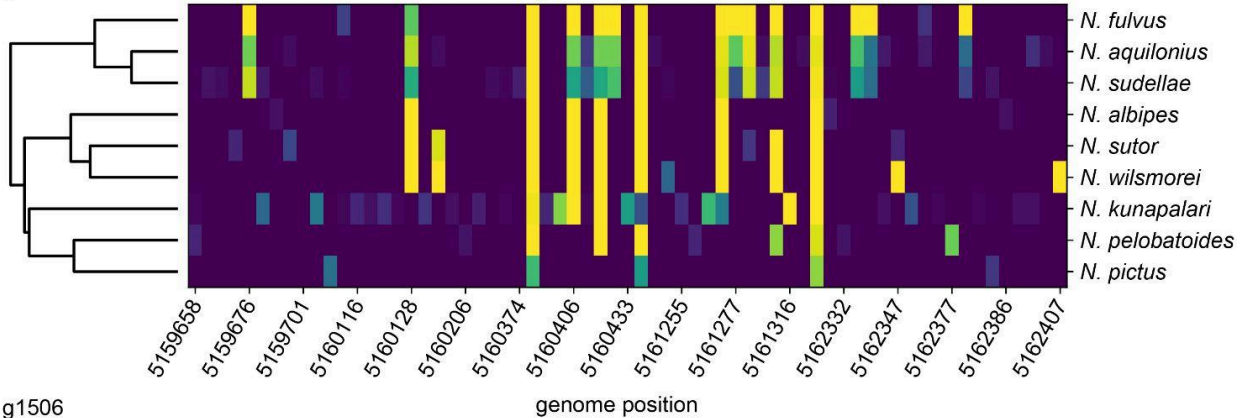


Supplementary Figure 6: Biallelic SNPs in CDS of genes under selection, colored and clustered by proportion of alternative allele per site per species (yellow: alternative allele is fixed in species; white: missing data in that species). [1-4 of 27]

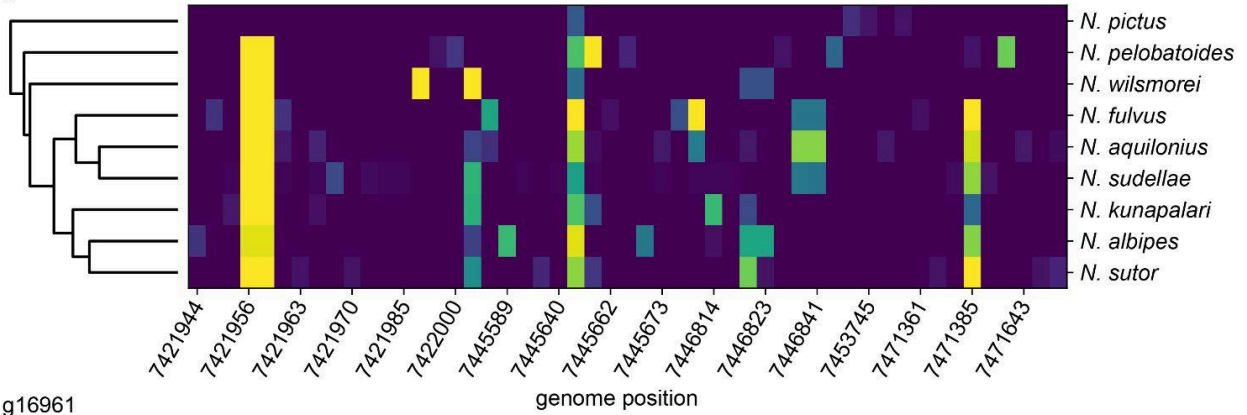
g1430



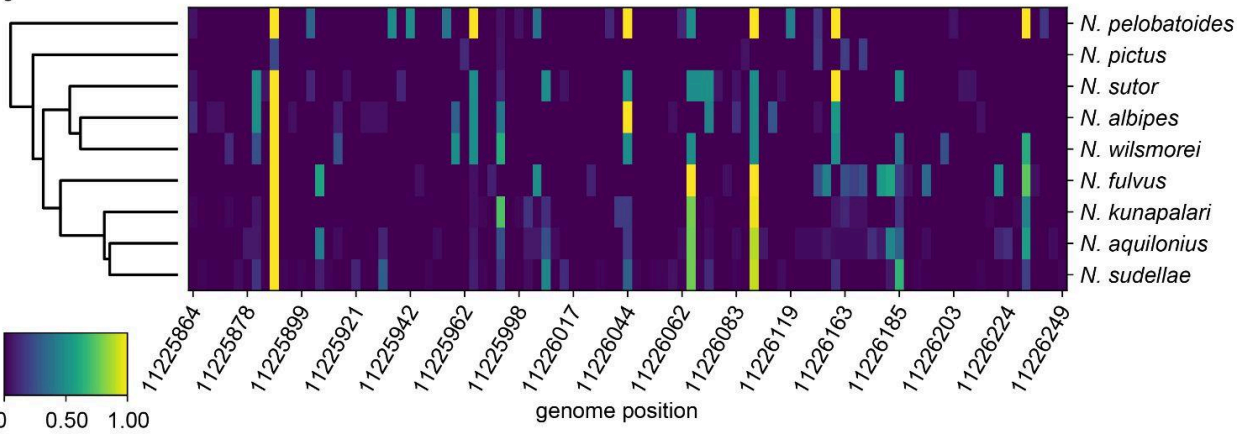
g1431



g1506



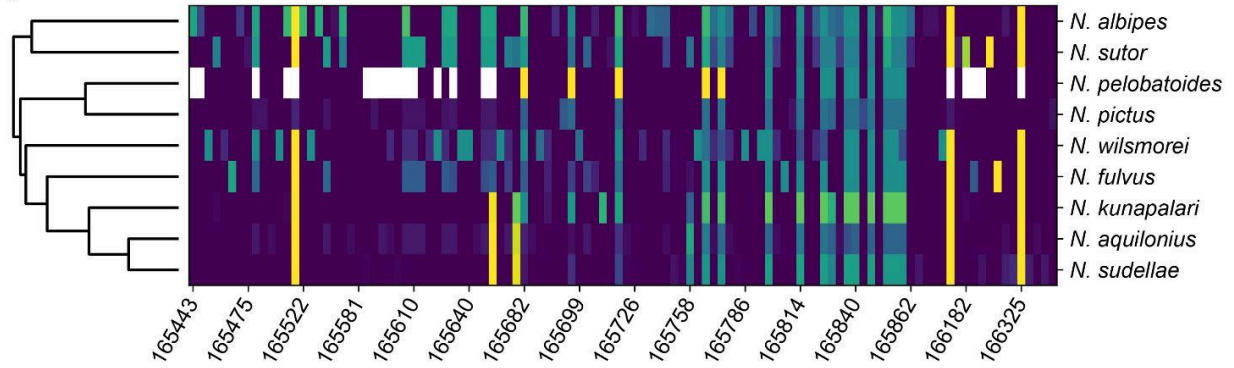
g16961



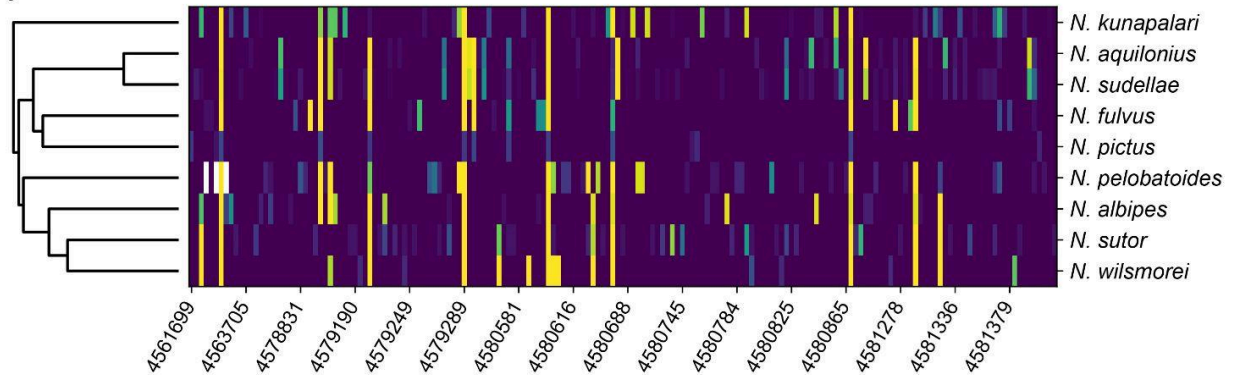
0 0.50 1.00

Supplementary Figure 6 cont.: Biallelic SNPs in CDS of genes under selection, colored and clustered by proportion of alternative allele per site per species (yellow: alternative allele is fixed; white: missing data in that species). [5-8 of 27]

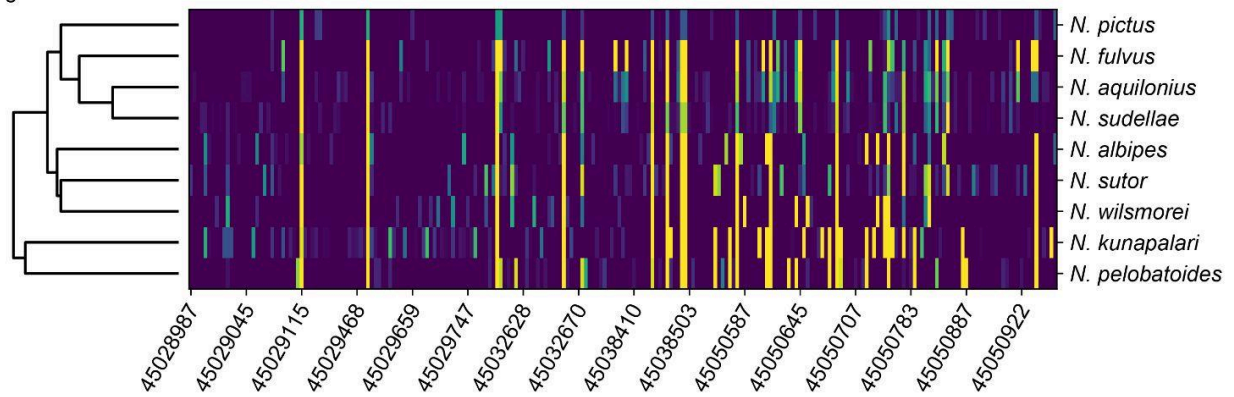
g18887



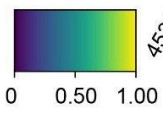
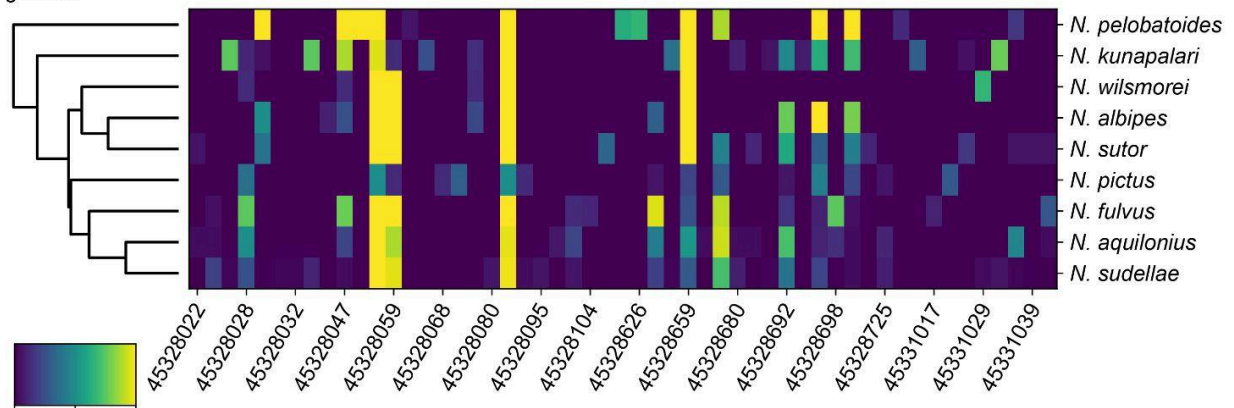
g22785



g23295

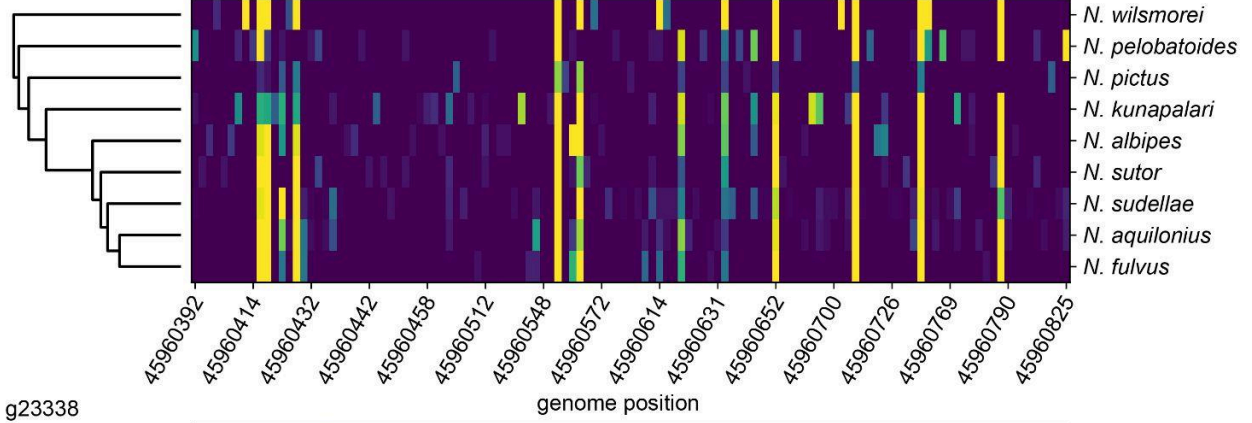


g23303

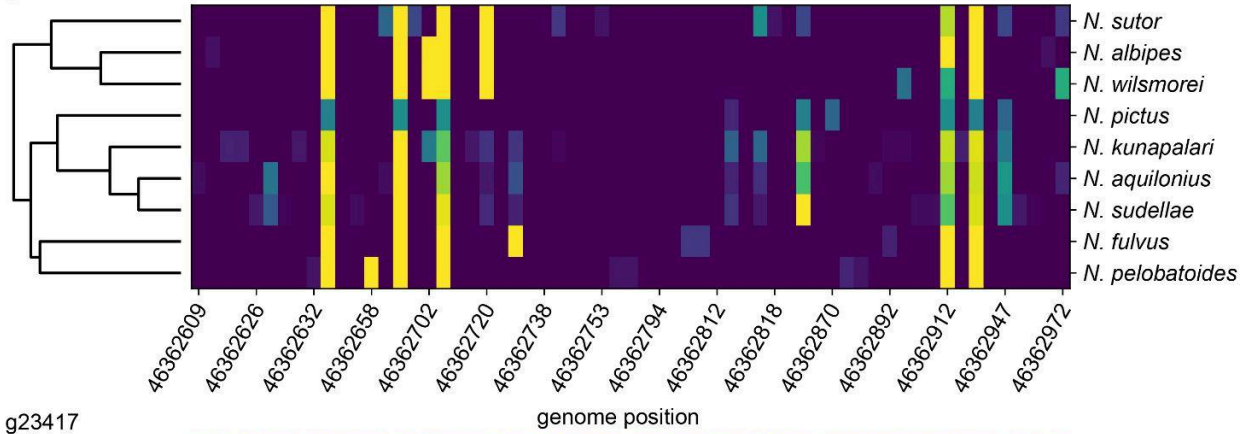


Supplementary Figure 6 cont.: Biallelic SNPs in CDS of genes under selection, colored and clustered by proportion of alternative allele per site per species (yellow: alternative allele is fixed; white: missing data in that species). [9-12 of 27]

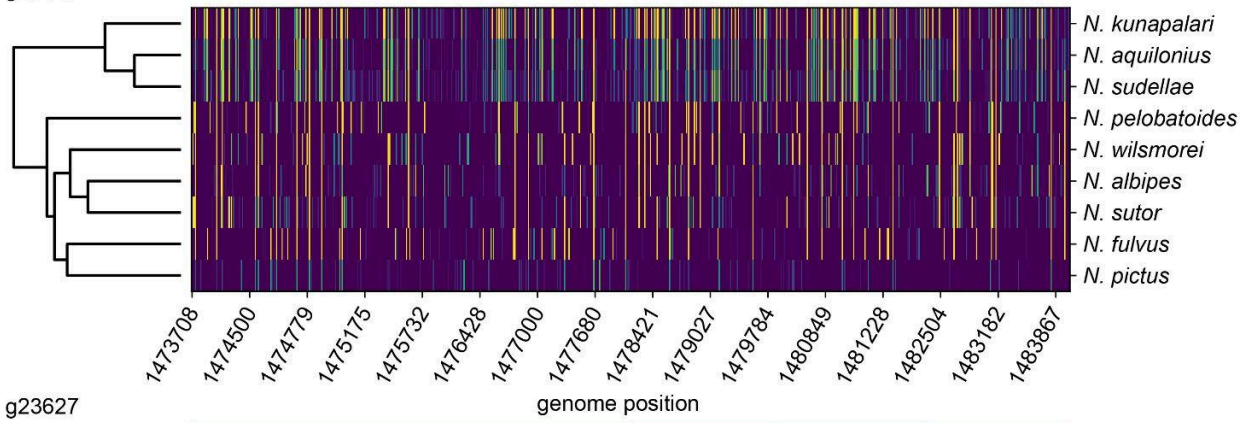
g23322



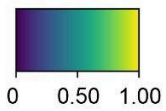
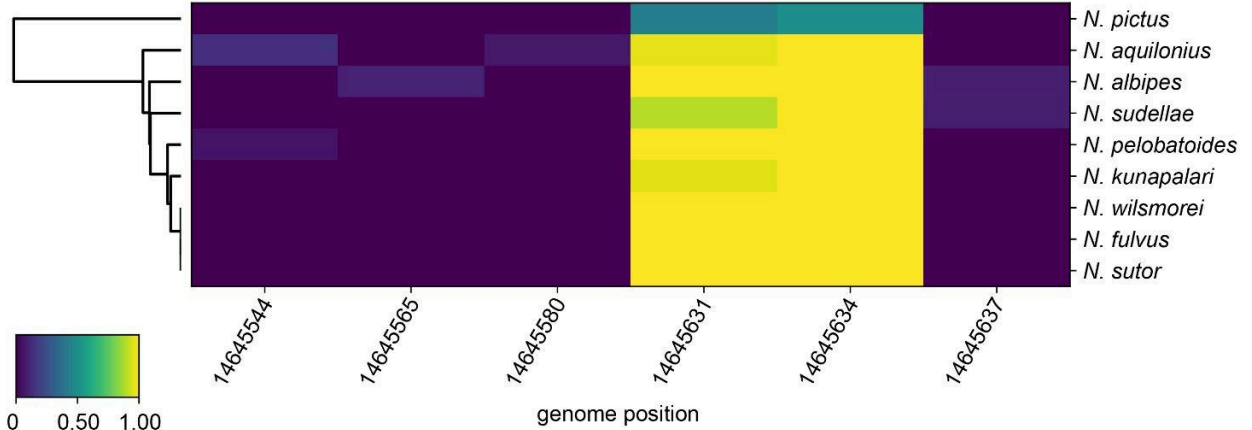
g23338



g23417

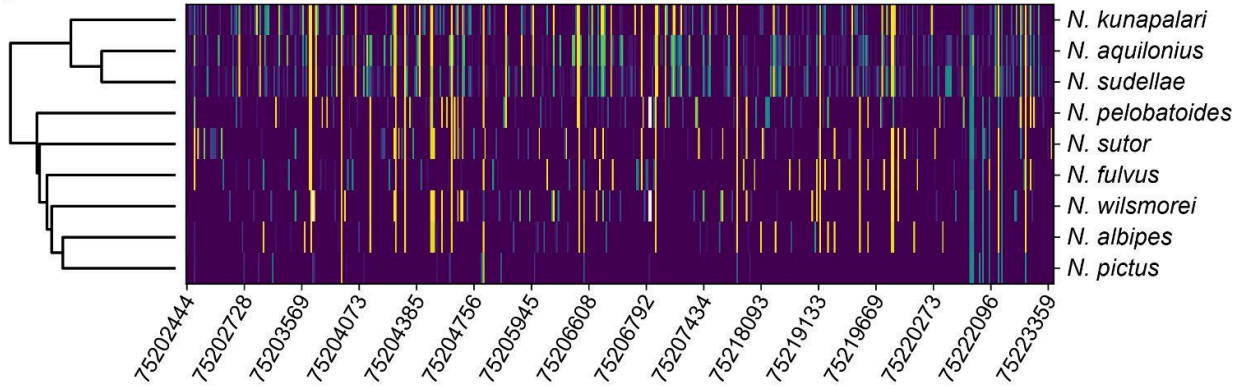


g23627

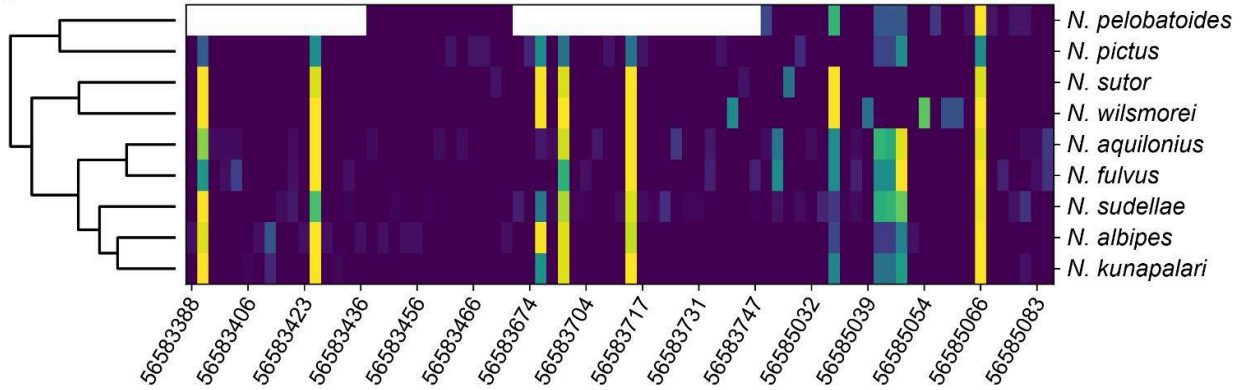


Supplementary Figure 6 cont.: Biallelic SNPs in CDS of genes under selection, colored and clustered by proportion of alternative allele per site per species (yellow: alternative allele is fixed; white: missing data in that species). [13-16 of 27]

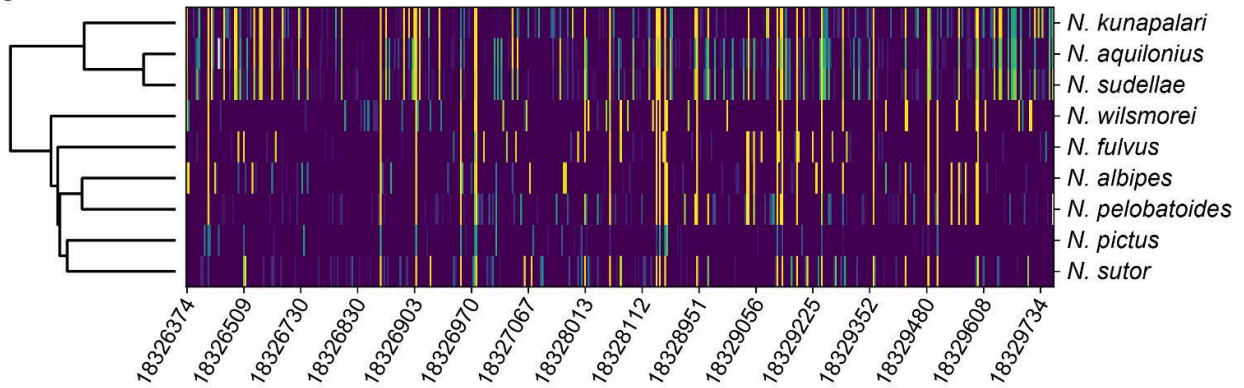
g2400



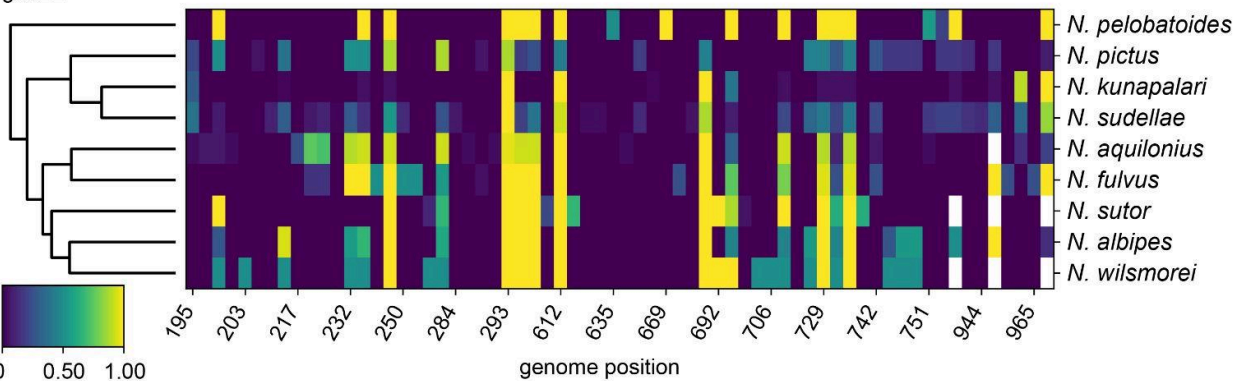
g3616



g5068

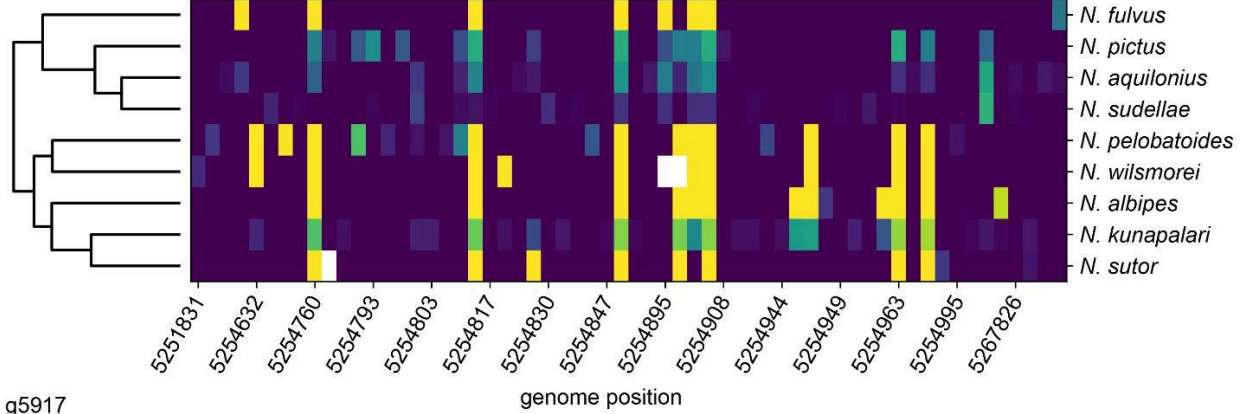


g5622

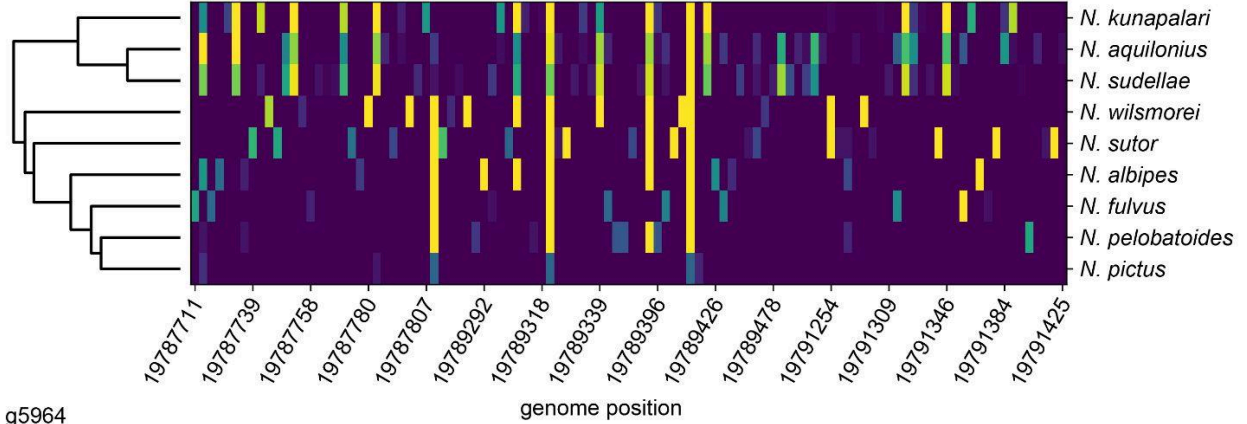


Supplementary Figure 6 cont.: Biallelic SNPs in CDS of genes under selection, colored and clustered by proportion of alternative allele per site per species (yellow: alternative allele is fixed; white: missing data in that species). [17-20 of 27]

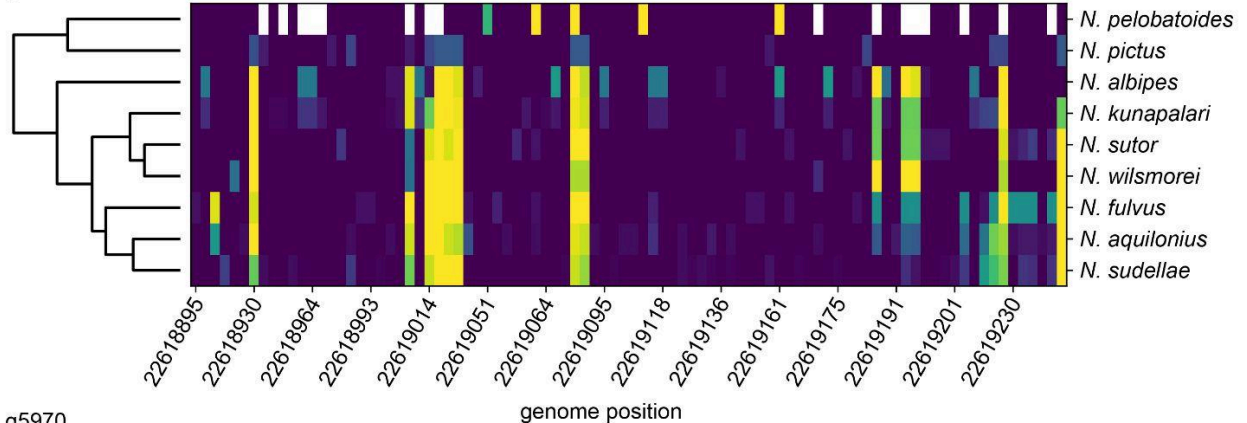
g5727



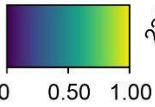
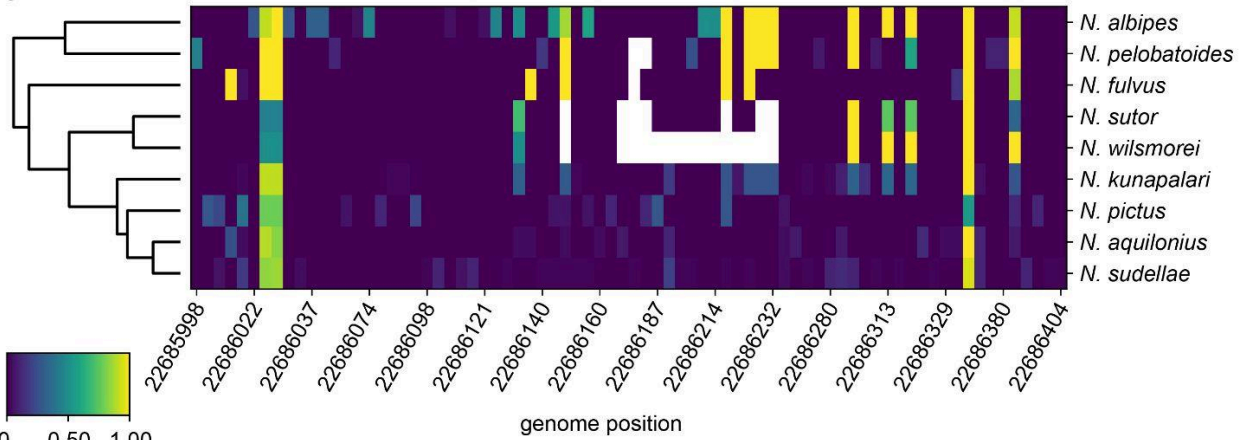
g5917



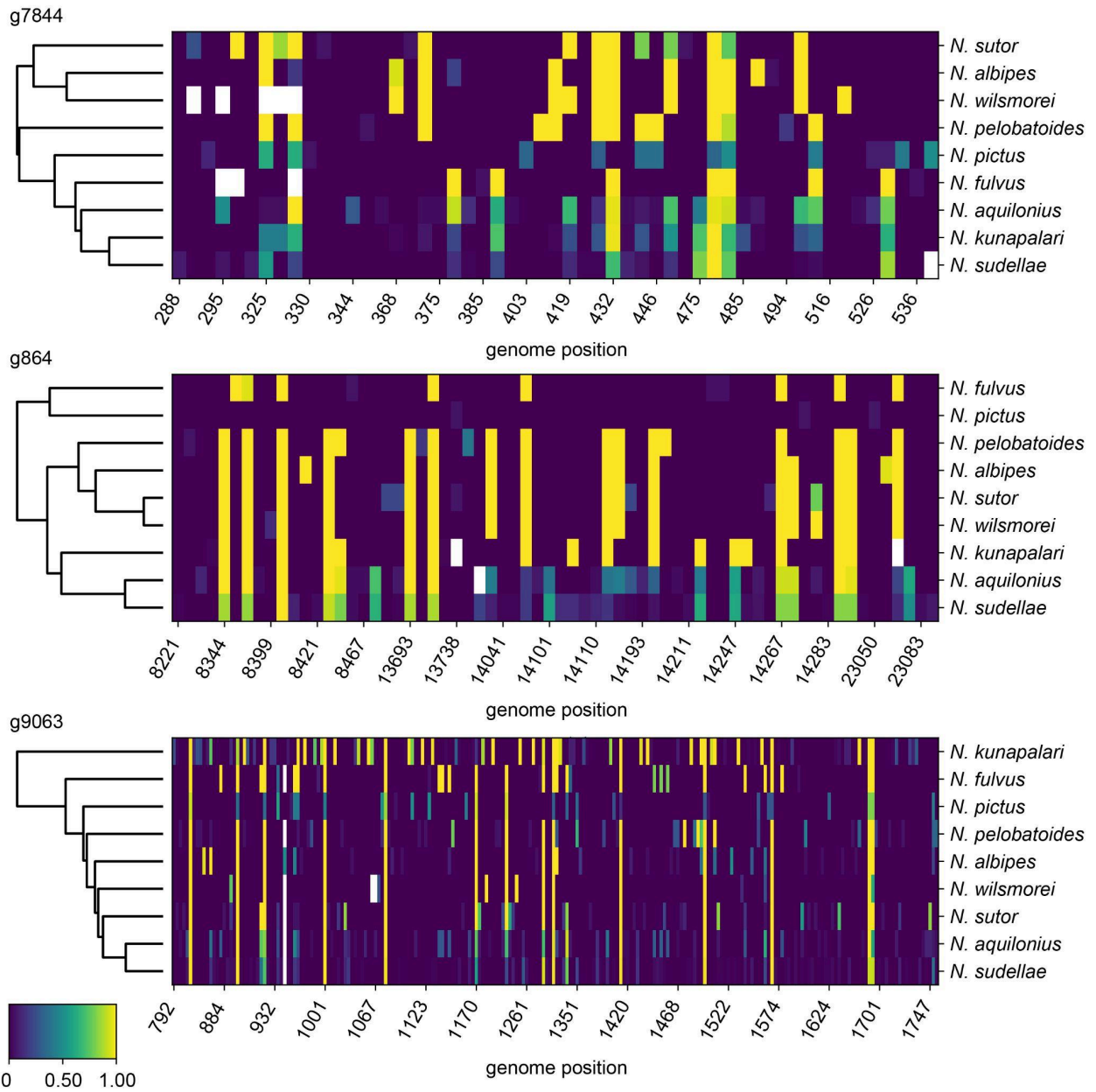
g5964



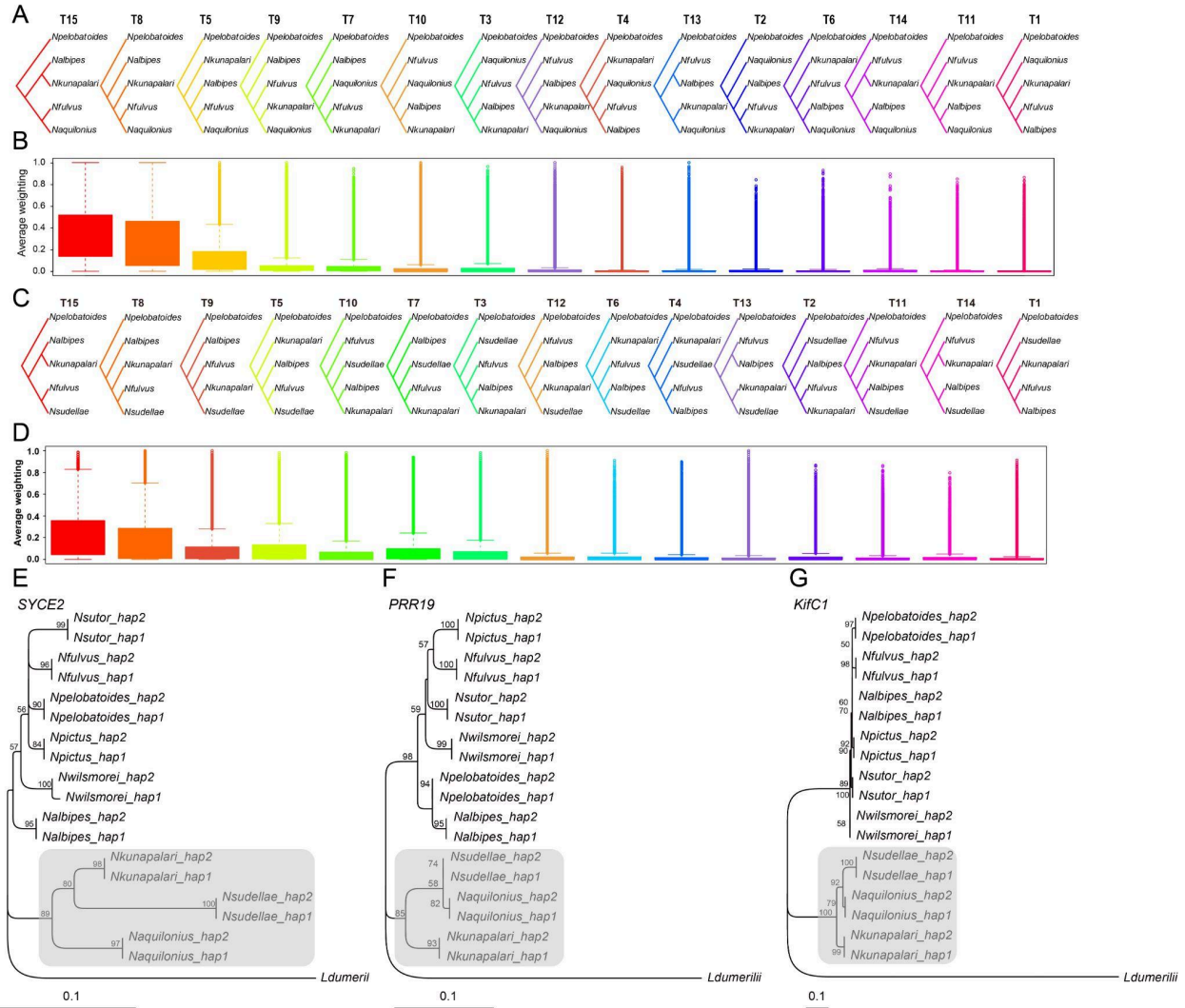
g5970



Supplementary Figure 6 cont.: Biallelic SNPs in CDS of genes under selection, colored and clustered by proportion of alternative allele per site per species (yellow: alternative allele is fixed; white: missing data in that species). [21-24 of 27]



Supplementary Figure 6 cont.: Biallelic SNPs in CDS of genes under selection, colored and clustered by proportion of alternative allele per site per species (yellow: alternative allele is fixed; white: missing data in that species). [25-27 of 27]



Supplementary Figure 7.: Topologies scans among tetraploids and candidate-gene phylogenies based on true haplotypes. A, C, The 15 possible rooted topologies for the two five-taxon datasets used in topology weighting analyses, with *N. pelobatooides* as the outgroup. The first dataset examines tetraploid relationships involving *N. kunapalari* and *N. aquilonius* (A), and the second examines relationships involving *N. kunapalari* and *N. sudellae* (C). B, D, Boxplots showing the genome-wide distribution of topology weighting for each topology shown in A and C, respectively. Introgression topologies 9, 12, and 13 showed the strongest support and were therefore summed in downstream analyses (Fig. 3F, G) to represent introgression phylogenetic signals among tetraploids. E–G, True haplotype gene trees for *SYCE2*, *PRR19*, and *KifC1*, reconstructed from 18 linked-read genome assemblies representing six diploid and three tetraploid species. The grey shaded boxes highlight the clade containing the three tetraploid species.